

Proc. of the 15th Int. Workshop on Slow Positron Beam Techniques and Applications, Prague, September 2–6, 2019

High Stability Positron Beam Generation Based on Ultra-intense Laser

F. LEI^a, J. JING^{a,*}, M. YAN-YUN^a, Z. ZI-JIA^a, L. YI-FEI^b, T. JUN-HAO^b, F. JIE^b,
Z. CHANG-QING^b, C. LI-MING^b, L. SONG^c AND N. HAFZ^c

^aDepartment of Physics, National University of Defense Technology, Changsha. 410073, China

^bInstitute of Physics CAS, Beijing, 100190, China

^cParticle and Terahertz Sources Division, ELI-ALPS, ELI-HU Non-Profit, Ltd., H-6720 Szeged, Hungary

Relativistic positron beams were generated by laser wakefield electrons bombarding on solid target. Very stable positron beams were generated in our experiments. The total yield of positrons is about 4.4×10^8 /shot. The energy spectra of positrons and electrons obey quasi-Maxwell distribution. Compared with the direct method, the indirect method produces positrons (38.5 MeV) and electrons (50.5 MeV) with much higher slope temperature.

DOI: [10.12693/APhysPolA.137.156](https://doi.org/10.12693/APhysPolA.137.156)

PACS/topics: 52.38.Kd, 52.59.-f, 25.20.-x

1. Introduction

Relativistic positron beam is one kind of important particle beam, which is widely used in nuclear physics, particle physics, and laboratory astrophysics [1]. There are three main traditional methods to generate positrons. The first one uses radioactive isotope β^+ decay [2]. Generally, long half-life nuclides, such as ^{22}Na , are used to generate slow positron beams. The intensity of the slow positron beams generated by this method is low and it is difficult to exceed 10^6s^{-1} . The second one is based on reactor [3]. The short-lived radioisotopes, such as ^{64}Cu , are activated by reactor to generate positrons through β^+ decay. Alternatively, Cd target is used, after capture of the thermal neutron, to emit high energy gamma rays. Then the gamma rays generate positrons by pair production. For example, the NEutron-induced POsitrone source MUniCh (NEPOMUC) can generate positron beams ($E = 15\text{--}1000\text{ eV}$) with intensity between $4 \times 10^7\text{ s}^{-1}$ and $5 \times 10^8\text{ s}^{-1}$, which is nowadays the most intensive positron source [4]. Thirdly, using traditional accelerators to accelerate electrons, positrons can be generated by high-energy electrons bombarding high Z target [5]. This method significantly improves positron beam intensity, but the accelerator costs are high and the floor space is large.

The generation of positron beams by ultra-intense laser has the characteristics of high beam intensity and low cost. There are two methods to generate positrons by laser. The first one is the direct method [6, 7]. Laser irradiates a solid target directly to generate hot electrons (about several MeV) on the target surface. Then these hot electrons interact with the target and generate

positrons. The second one is the indirect method [8, 9]. Laser first interacts with a gas target to accelerate electrons by laser wakefield acceleration (LWFA), then these energetic electrons (about hundreds of MeV) interact with a solid target and generate positrons. In recent years, great development has been made in electron acceleration experiments by LWFA. The electron energy is constantly increasing, and the maximum electron energy has reached GeV. The rapidly increasing electron energy has made positron generated by ultra-intense laser more and more attractive. There are two processes to generate positrons in the electrons-matter interactions [10]

$$e^- + Z \rightarrow e^- + e^+ + Z, \quad (1)$$

$$e^- + Z \rightarrow \gamma + Z, \quad \gamma + Z \rightarrow e^- + e^+ + Z \quad (2)$$

Equation (1) is the Trident process. Positrons are generated directly by the interactions of electrons and target nuclei, with positron yield $N_{e^+} \propto Z^2/A$. Equation (2) is the Beth-Heitler process. High-energy photons are produced first when electrons interact with nuclei, and then positrons are generated in the Coulomb field of nuclei by pair effects, with positron yield $N_{e^+} \propto (Z^2/A)^2$ [8, 11].

2. Experimental layout

Figure 1 shows the experimental layout of the indirect method. The experiments were carried out on the 200TW laser of Shanghai Jiaotong University. The laser wavelength is $\lambda_L = 800\text{ nm}$, the energy is $E_L = 3.2\text{ J}$ and the duration is $\tau_L = 30\text{ fs}$. Laser beam focused on the edge of a 2 mm long slit-shaped gas jet. The gas is N_2 with pressure of 3 bar. Laser focal spot accounts for 30% of total energy within $30\text{ }\mu\text{m}$ radius. The peak laser intensity is $I_L \simeq 2.3 \times 10^{18}\text{ W/cm}^2$. The target material is W ($Z=74$) with thickness of 4 mm, which is a good exchange for positron generation. The hole of collimator is 10 cm long and 1 cm in

*corresponding author; e-mail: jiang-jing.68@163.com

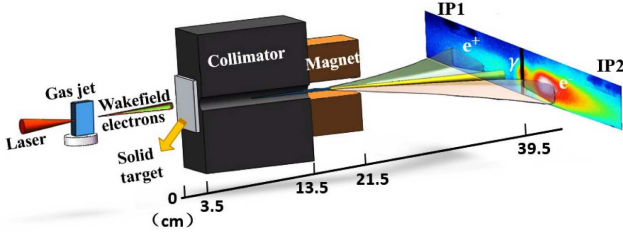


Fig. 1. Experiment layout.

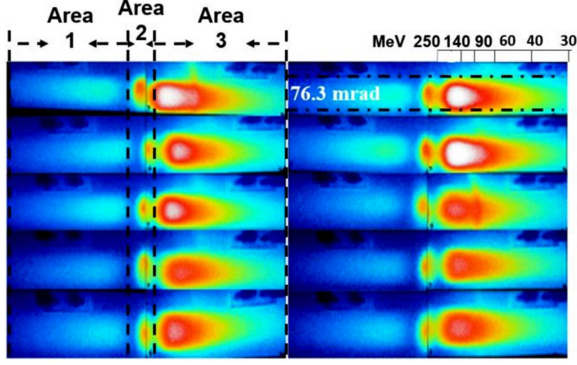


Fig. 2. IP signals of ten groups experiments.

diameter. The strength of the permanent dipole magnet is about 0.9 T. Two IPs (Image Plate) were placed parallel 39.5 cm away from the solid target. Five shots in a group were used to get an obvious positron signal in our experiments. Ten groups were conducted.

3. Experimental results

3.1. Positron yield

Figure 2 shows the signals on IPs, and it is clear that these signals are divided into three parts. Area 1 is positron signal, area 2 is photon signal, and area 3 is electron signal. Positron yields of ten groups are shown in Table I. The average positron yield is 6.81×10^6 /shot, and the standard deviation of positron yield is 2.92×10^6 /shot. The positron yield of each group has exceeded 3×10^6 /shot, which indicates that the positron beams are very stable and can be used as high-energy particle sources for other studies [1]. Figure 3 shows the wakefield electron signal and the wakefield electron spectrum without solid target. By inserting the electron spectrum into the Monte Carlo code FLUKA [12], the comparison between the simulation results and experimental results are shown in Fig. 4. The simulation results are in good agreement with experimental results. For simulation results, the total yield of positrons generated ($E > 1$ MeV in full space) behind the solid target is about 65 times the number of positrons ($30 \text{ MeV} < E < 250 \text{ MeV}$ in 4.6 msr solid angle behind the target) that can reach the IPs, so the average total yield of positrons in full space in our experiments is about 4.4×10^8 /shot.

 TABLE I
 Positron yield of each group per shot. Average value is 6.81.

| Group | Positron yield $\times 10^6$ | Group | Positron yield $\times 10^6$ |
|-------|------------------------------|-------|------------------------------|
| 1 | 5.2 | 6 | 4.8 |
| 2 | 8.2 | 7 | 3.9 |
| 3 | 10.0 | 8 | 3.2 |
| 4 | 9.7 | 9 | 6.7 |
| 5 | 11.7 | 10 | 4.7 |

These positron yield refers to the positrons received by IPs, whose energy is $30 \text{ MeV} < E < 250 \text{ MeV}$ in 4.6 msr solid angle behind the target.

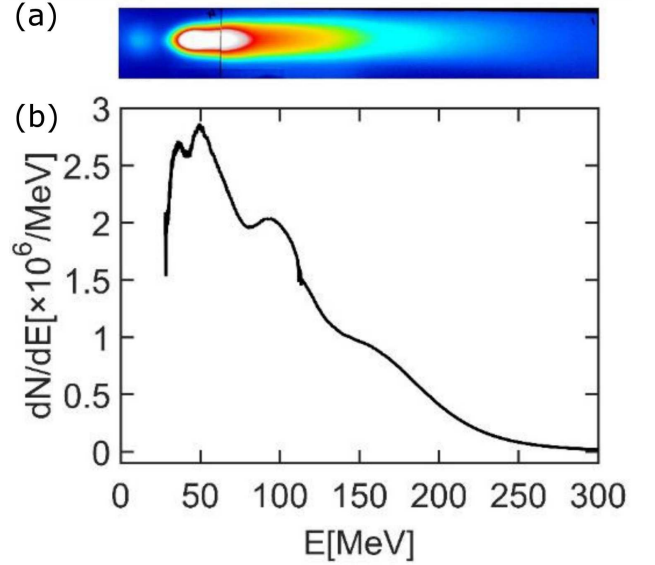


Fig. 3. (a) The IP signals of wakefield electrons. (b) The energy spectrum of wakefield electrons.

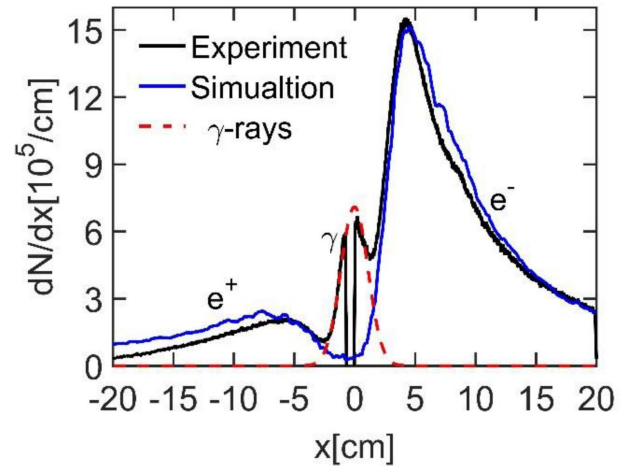


Fig. 4. Comparisons between experimental results and simulation results.

3.2. The energy spectra of positrons and electrons

The energy spectra of positrons and electrons are shown in Fig. 5. It is noteworthy that there are two obvious signal peak at $x = 4.3$ cm and $x = -6.0$ cm (the corresponding energy is 112 MeV and 81 MeV) in Fig. 4, where the number of electrons and positrons received is more than that elsewhere, but this feature is not found in Fig. 5. The reason is that the calibration energy of electrons and positrons shown in Fig. 6 varies dramatically with the location of IPs.

In our experiment, the energy spectra of positrons and electrons satisfy the quasi-Maxwell distribution, as shown in Fig. 5. The slope temperatures of positrons and electrons are 38.5 MeV and 50.5 MeV, respectively. Compared with 2.8 MeV and 4.8 MeV, measured by Chen in the direct method [7], the indirect method produces positrons and electrons with much higher temperature.

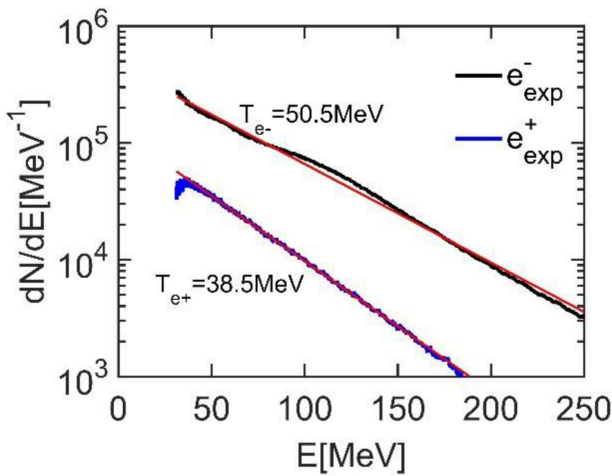


Fig. 5. The energy spectra of electrons and positrons.

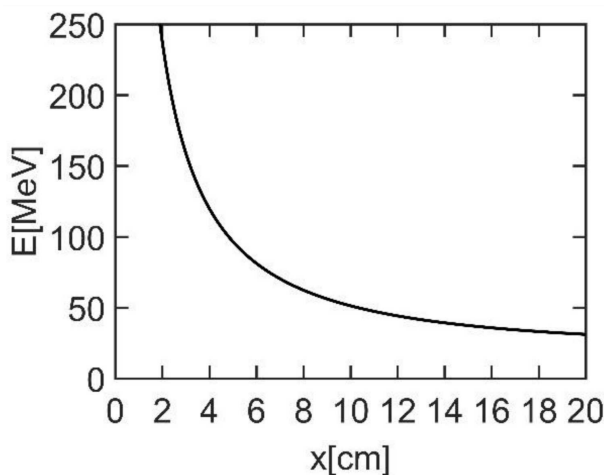


Fig. 6. The energy calibration of electrons and positrons on IPs.

In Chen's paper [7], the measured temperature of positrons is about half that of electron temperature (the temperature ratio is about 0.58), and the explanation is as follows: a source electron produced by laser distributes its energy to the newly created positron and electron. Therefore, the positron is expected to obtain half energy of the source electron. But in the indirect method, the measured temperature ratio of positrons to electrons in our experiment is about 0.76. The fundamental reason for the different temperature ratio of positrons to electrons generated by the two methods is due to the largely different conversion efficiency of source electrons. In the direct method, compared with wakefield electrons, the energy of hot electrons is so small that only a few hot electrons can generate new positrons and electrons by the Trident process and B-H process. The obvious phenomenon is that the number of electrons measured behind the target is two orders of magnitude higher than that of positrons, while the number of electrons in the indirect method is only 5.1 times that of positrons. When the thickness of solid target is increased, the number and temperature of positrons and electrons will tend to become same. In this case, the neutral electron-positron pair plasmas may be produced [9].

4. Summary

Through the interactions between the ultra-intense laser and gas-solid target, positron beams can be generated very stably. The total yield of positrons generated is about 4.4×10^8 /shot. The energy spectra of electrons and positrons satisfy quasi-Maxwell distributions, and the slope temperatures are 50.5 MeV and 38.5 MeV, respectively. Compared with the direct method, the indirect method produces positrons and electrons with much higher temperature, and due to the high conversion efficiency of the wakefield electrons for generating positrons, the temperature ratio of electrons to positrons behind the target is also quite different.

Acknowledgments

This work was supported by the National Natural Science Foundation of China (Grant Nos. 11975308, 11690040, 11675107, and 11690043), the Science Challenge Project (Grant No. TZ2019001).

References

- [1] A. Pukhov, M. Yer-Vehn, *J. Appl. Phys. B*, **4**, 74 (2002).
- [2] X. Guo, T. Huang, *Chin. Phys. Lett.*, **8**, 6 (1991).
- [3] A. Van Veen, F. Labohm, H. Schut, et al., *Appl. Surf. Sci.*, **2**, 116 (1997).
- [4] C. Hugenschmidt, G. Dollinger, W. Egger, et al., *Appl. Surf. Sci.*, **1**, 255 (2008).
- [5] T. Akahane, T. Chiba, N. Shiotani, et al., *Appl. Phys. A*, **2**, 51 (1990).

- [6] H. Chen, S.C. Wilks, D.D. Meyerhofer, et al. *Phys. Rev. Lett.* **105**, 15003 (2010).
- [7] H. Chen, S.C. Wilks, J.D. Bonlie, et al., *Phys. Rev. Lett.* **102**, 105001 (2009).
- [8] G. Sarri, W. Schumaker, P.A. Di, et al. *Phys. Rev. Lett.* **110**, 25502 (2013).
- [9] G. Sarri, K. Poder, J.M. Cole, et al. *Nat. Commun.* **6**, 6747 (2015).
- [10] K.I. Nakashima, H. Takabe *Phys. Plasmas* **9**, 1505 (2002).
- [11] C. Hugenschmidt, B. Lowe, J. Mayer, et al., *Nucl. Instrum. Methods Phys. Res. A.* **3**, 593 (2008).
- [12] G. Battistoni, F. Cerutti, A. Fassó, A. Ferrari, S. Muraro, J. Ranft, S. Roesler, P.R. Sala, *AIP Conf. Proc.* **896**, 31 (2007).